Embedded-atom-method effective-pair-interaction study of the structural and thermodynamic properties of Cu-Ni, Cu-Ag, and Au-Ni solid solutions

Mark Asta and Stephen M. Foiles
Computational Materials Science Department, Sandia National Laboratories, P.O. Box 939, MS 9163, Livermore, California 94551-0939
(Received 14 July 1995; revised manuscript received 5 October 1995)

The structural and thermodynamic properties of Cu-Ni, Cu-Ag, and Au-Ni solid solutions have been studied using a computational approach which combines an embedded-atom-method (EAM) description of alloy energetics with a second-order-expansion (SOE) treatment of compositional and displacive disorder. It is discussed in detail how the SOE approach allows the EAM expression for the energy of a substitutional alloy to be cast in the form of a generalized lattice-gas Hamiltonian containing effective pair interactions with arbitrary range. Furthermore, we show how the SOE-EAM method can be combined with either mean-field or Monte Carlo statistical mechanics techniques in order to calculate short-range-order (SRO) parameters, average nearest-neighbor bond lengths, and alloy thermodynamic properties which include contributions from static displacive relaxations and dynamic atomic vibrations. We demonstrate that the contributions to alloy heats of mixing arising from displacive relaxations can be sizeable, and that the neglect of these terms can lead to large overestimations of calculated phase-transition temperatures. The effects of vibrational free-energy contributions on the results of composition-temperature phase diagram calculations are estimated to be relatively small for the phase-separating alloy systems considered in this study. It is shown that within the SOE approach displacive effects can act only to displace the peak in the Fourier-transformed SRO parameter away from Brillouin-zone-boundary special points and towards the origin. Consistent with this result, we show that the unusual SRO observed in diffuse scattering experiments for Au-Ni solid solutions can be understood as arising from a competition between chemical and displacive driving forces which favor ordering and clustering, respectively.

I. INTRODUCTION

Solid solutions form the most commonly occurring class of alloy phases in the solid state. These phases are challenging to study both theoretically and experimentally due to the topological and configurational disorder associated with their atomic structures. In the past 30 years, a number of theoretical techniques have been developed which make possible computational studies of the structural and thermodynamic properties of alloy solid solutions.[1–9] These approaches vary in the manners in which they treat the computational complexities associated with the structural disorder in alloys. In one approach employed in a number of theoretical studies,[1,2,9] use is made of a second-order expansion (SOE) of the energy with respect to atomic displacements and site-occupation variables. The result of such an expansion is an expression for the energy of a substitutional alloy which has a form analogous to the Hamiltonian of a lattice-gas model. In this paper we present results of a computational study which combines the formalism of a SOE approach with a description of alloy energetics based on the embedded atom method (EAM).[10,11]

The EAM is a semiempirical, interatomic-potential method which has been applied widely to the study of structural and thermodynamic properties of crystalline materials, liquids, surfaces, and defects.[11] The EAM has proven to be successful particularly in describing the properties of noble and late transition metals and their alloys. In the current study the combined SOE-EAM approach has been used in combination with mean-field (MF) statistical mechanics calculations and Monte Carlo (MC) simulations[12] in order to compute structural and thermodynamic properties of the solid-solution phases of Cu-Ni, Au-Ni, and Cu-Ag. Particular attention has been devoted to computing the magnitudes of local atomic displacements and to studying the effects which these displacements have on calculated values of the heats of mixing, composition-temperature (c-T) phase diagrams, and short-range-order (SRO) parameters.

Vibrational (phonon) contributions to the free energy are often neglected in computational studies of the thermodynamic properties of alloys. The results of a number of theoretical (see Refs. 13–18 and references therein) and experimental[19] studies have demonstrated that these contributions may be sizable and that they can have important consequences for alloy phase transitions. In the present work we have developed an approximate method for computing vibrational free energies of disordered alloys within the SOE framework. With this method the effects which vibrational free-energy contributions have on calculated c-T phase diagrams have been assessed.

A source of motivation for the present work is provided by the fact that the SOE-EAM approach combined with MF statistical mechanics provides a method for computing alloy thermodynamic properties which offers the following computational advantages over direct MC-based calculations: It is significantly faster and it allows one to avoid statistical uncertainties associated with MC simulations. We are therefore interested in assessing the accuracy of both the SOE and MF approximations. In this paper we will discuss the accuracy of the SOE treatments of alloy energetics and atomic vibrations by comparing to results of more exact, direct cal-

culations which we have performed within the context of the EAM. Additionally, the values of thermodynamic properties and SRO parameters calculated by MF and MC simulations will be compared in order to estimate the magnitudes of the errors associated with the MF approximation. The issues of accuracy discussed in this paper should be of general interest because both the MF approximation and the basic SOE formalism have been and continue to be used widely in computational studies of alloy structural and thermodynamic properties.

II. COMPUTATIONAL APPROACH

In this section we describe the SOE approach to treating compositional and displacive disorder in crystalline solid solutions. Additionally, we discuss how this approach can be used in MF calculations and MC simulations in order to study structural as well as finite-temperature, thermodynamic properties. The basic formalism described in this section was discussed in detail previously by de Fontaine[1] and it shares many features in common with the method of de Gironcoli *et al.*[9]

In the discussion which follows we present details of the application of the SOE approach to systems of interest in this paper, namely, solid solutions of binary (A-B) alloys where the parent lattice has cubic and inversions symmetries with one atomic site per unit cell. Additionally, we describe in detail how the SOE method can be implemented in the special case where the alloy energetics are parametrized by EAM potentials. The extension of the formalism presented below to multicomponent alloy systems and to lattices with lower symmetry is straightforward in principle (the details of the formalism in the case of multicomponent alloys may be found in Refs. 1 and 7). The underlying formalism is not limited in its application to EAM potentials alone; details of the implementation within the context of pair potentials,[1] pseudopotential-linear-response[9] theory, and all-electron methods[7,8] are given elsewhere.

A. Second-order energy expansion

Typically, the arrangement of atoms in a crystalline alloy solid solution can be described with reference to a so-called ''parent'' lattice, the crystallographic sites of which coincide with average atomic positions. The positions of the atoms can be specified with reference to the sites of the parent lattice through the use of two types of variables. The first is an occupation variable $c(\mathbf{R})$, which is equal to 1 or 0 depending on whether an A or B atom is associated with the lattice site located at $\mathbf{R}$, respectively. Additionally, the displacement vector $\mathbf{u}(\mathbf{R})$ gives the position of the atom relative to the lattice site at $\mathbf{R}$. The energy of a given arrangement of atoms is a function of the set of occupation variables, displacement vectors, and the atomic volume Ω: $E(\{c(\mathbf{R})\},\{\mathbf{u}(\mathbf{R})\},\Omega)$.

In the SOE approach, the energy at fixed volume is expanded to second order in the compositional and displacement variables. This expansion is formulated with respect to a reference state, which can be defined in a number of ways. Two choices for the reference state used in previous work are the following: (1) the ''host'' reference state[2] corresponding to an elemental, crystalline solid of the majority alloy constituent where $c(\mathbf{R})=\mathbf{u}(\mathbf{R})=0\ \forall\ \mathbf{R}$, and (2) a homogeneous, unrelaxed, *equiatomic*, random alloy[9] characterized by $c(\mathbf{R})=1/2$ and $\mathbf{u}(\mathbf{R})=0\ \forall\ \mathbf{R}$. An alternative choice, which is introduced in Ref. 1, is a reference state defined in terms of the average composition (c) as follows: $c(\mathbf{R})=c$ and $\mathbf{u}(\mathbf{R})=0\ \forall\ \mathbf{R}$, where c is the value of $c(\mathbf{R})$ averaged over all lattice sites. With this latter choice of reference state, the Taylor series expansion of the energy to second order has the form

$$E(\{c(\mathbf{R})\},\{\mathbf{u}(\mathbf{R})\},\Omega)=E_0+\frac{1}{2}\sum_{\mathbf{R},\mathbf{R}'}\left[\theta(\mathbf{R}-\mathbf{R}')\,\delta c(\mathbf{R})\,\delta c(\mathbf{R}')+2\psi_\alpha(\mathbf{R}-\mathbf{R}')\,\delta c(\mathbf{R})u_\alpha(\mathbf{R}')+\phi_{\alpha,\beta}(\mathbf{R}-\mathbf{R}')u_\alpha(\mathbf{R})u_\beta(\mathbf{R}')\right]. \quad (1)$$

In the expansion (1) the first-order terms vanish due to the translational and inversion symmetries of the reference state and due to the fact that the sum over all lattice sites of $\delta c(\mathbf{R})\equiv c(\mathbf{R})-c$ is zero by definition. In Eq. (1) (and in those which follow) sums over repeated Cartesian indices α and β are implied. It should be noted that E_0, θ, ψ_α, and $\phi_{\alpha,\beta}$ are all composition- and volume-dependent quantities. E_0 denotes the energy of the homogeneous reference state. $\theta(\mathbf{R}-\mathbf{R}')$ is the second derivative of the energy with respect to the occupation variables at $\mathbf{R}$ and $\mathbf{R}'$ (evaluated in the reference state). ψ_α, the mixed second derivative with respect to occupation variables and displacement vectors, is referred to as the solute-lattice coupling parameter.[1] The product $\psi_\alpha(\mathbf{R}-\mathbf{R}')\delta c(\mathbf{R})$ is the α component of the force at $\mathbf{R}'$, which arises from a deviation of the occupation variable from its average value at $\mathbf{R}$. $\phi_{\alpha,\beta}$ is the force-constant matrix corresponding to the homogeneous reference state.

The equilibrium (also called *static*) displacements $\mathbf{u}^0(\mathbf{R})$ associated with a given set of occupation variables can be obtained by setting equal to zero the partial derivative of Eq. (1) with respect to $u_\alpha(\mathbf{R})$:

$$u^0_\alpha(\mathbf{R})=-\sum_{\mathbf{R}',\mathbf{R}''}\phi^{-1}_{\alpha,\beta}(\mathbf{R}-\mathbf{R}')\psi_\beta(\mathbf{R}'-\mathbf{R}'')\,\delta c(\mathbf{R}''). \quad (2)$$

When the set of formulas for the equilibrium displacements is inserted into Eq. (1), a simplified expression for the energy can be derived which has the following form, written in $\mathbf{k}$ space:

$$E = E_0 + \frac{1}{2N}\sum_{\mathbf{k}} V(\mathbf{k})\,\delta c(\mathbf{k})\,\delta c^*(\mathbf{k}) + \frac{1}{2N}\sum_{\mathbf{k}} \phi_{\alpha,\beta}(\mathbf{k})\,\delta u_\alpha(\mathbf{k})\,\delta u^*_\beta(\mathbf{k}). \quad (3)$$

In Eq. (3), N is the number of atoms and $\delta u_\alpha(\mathbf{k}) \equiv u_\alpha(\mathbf{k}) - u^0_\alpha(\mathbf{k})$ denotes the Fourier transform of the deviation of $u_\alpha(\mathbf{R})$ from its equilibrium value. $V(\mathbf{k})$ is the Fourier transform of the so-called effective pair interaction (EPI), which is defined as

$$V(\mathbf{k}) = \theta(\mathbf{k}) - \psi_\alpha(\mathbf{k})\,\phi^{-1}_{\alpha,\beta}(\mathbf{k})\,\psi^*_\beta(\mathbf{k}). \quad (4)$$

From Eq. (4) we see that the EPI contains two contributions. The first describes the nature of the chemical interactions in the system, and the second is a *relaxation-energy* contribution associated with the static displacements. In Eq. (3) the sum of the first two terms on the right-hand side corresponds to the zero-temperature energy of a given configuration of atoms located at their equilibrium positions. The third term is a thermal one which determines the cost in energy associated with deviations in the locations of the atoms from their equilibrium positions.

An important point to note is that at $\mathbf{k}=0$ the force constant matrix (ϕ) is not invertible and the second term on the right-hand side of Eq. (4) is undefined. In the long-wavelength ($|\mathbf{k}|\rightarrow 0$) limit, $\psi(\mathbf{k})\phi^{-1}(\mathbf{k})\psi^*(\mathbf{k})$ is finite with a value which is given by continuum elasticity theory (see, e.g., Refs. 1 and 5). However, the value of $\psi\phi^{-1}\psi^*$ in this limit depends on the direction of approach to $\mathbf{k}=0$. The singularity of $V(\mathbf{k})$ at the origin poses no problem for what follows because the term $\mathbf{k}=0$ can be excluded from the first sum on the right-hand side of Eq. (3), since $\delta c(\mathbf{k}=0)=0$ by definition (owing to our choice of a concentration-dependent reference state).

B. Thermodynamic properties and short-range order

In the present study we are interested in the structural and thermodynamic properties and phase stability of alloy solid solutions. The structural properties with which we shall be concerned are the atomic SRO and the average nearest-neighbor pair distances for A-A, B-B, and A-B bonds. The SRO is quantified by values of the pair correlation functions (PCF's) $\langle \delta c(\mathbf{R})\delta c(\mathbf{R}')\rangle$ (or quantities such as the Warren-Cowley SRO parameters, which are proportional to them[1]), which give a measure of the tendency for atoms at sites $\mathbf{R}$ and $\mathbf{R}'$ to be preferentially occupied by like or unlike atom types. The average nearest-neighbor distance for A-A, A-B, and B-B pairs can be determined from the relative displacements δ_{AA}, δ_{AB}, and δ_{BB} defined as

$$\begin{aligned}
\delta_{AA}(\tau) &= \langle c(\mathbf{R}+\tau)\mathbf{u}^0(\mathbf{R}+\tau)\rangle - \langle c(\mathbf{R})\mathbf{u}^0(\mathbf{R})\rangle,\\
\delta_{AB}(\tau) &= \langle c(\mathbf{R}+\tau)\mathbf{u}^0(\mathbf{R}+\tau)\rangle - \langle [1-c(\mathbf{R})]\mathbf{u}^0(\mathbf{r})\rangle,\\
\delta_{BB}(\tau) &= \langle [1-c(\mathbf{R}+\tau)]\mathbf{u}^0(\mathbf{R}+\tau)\rangle - \langle [1-c(\mathbf{R})]\mathbf{u}^0(\mathbf{R})\rangle,
\end{aligned} \quad (5)$$

where τ is a vector connecting nearest-neighbor pairs in the parent lattice. By combining Eqs. (2) and (5) it is possible to define δ_{AA}, δ_{AB}, and δ_{BB} in terms of nearest-neighbor PCF's. Therefore, both SRO and average bond-length information can be obtained from a knowledge of the values of the PCF's.

The thermodynamic property directly related to the stability of an alloy solid solution under conditions of constant pressure and temperature is the Gibbs free energy of formation, defined as the difference between the alloy Gibbs free energy (G) and the concentration-weighted average of the values of G for the constituent element phases. For an alloy with an energy given by Eq. (3), G can be formally written as

$$G(N,c,T,P) = E_0 + \frac{1}{2N}\sum_{\mathbf{k}} V(\mathbf{k})\langle \delta c(\mathbf{k})\,\delta c^*(\mathbf{k})\rangle + \langle F_v(T,\Omega,\{c(\mathbf{R})\})\rangle - TS_c + NP\Omega, \quad (6)$$

where P is the pressure, T is the temperature, S_c is the configurational entropy, F_v is the vibrational free energy, and the brackets $\langle\ \rangle$ denote ensemble averages over the configurational degrees of freedom (i.e., the occupation variables). Consistent with Eq. (3), the expression for the vibrational free energy used in the present study corresponds to that of a quasiharmonic model where $\phi_{\alpha,\beta}$ form the elements of the volume-dependent force-constant matrix. In this work we are interested in estimating the vibrational contribution to the free energy of solid-solution phases for values of T well above the measured Debye temperatures of the constituent elemental solids. Consequently, we will make use of the high-temperature limit of the expression for the vibrational free energy of a quasiharmonic model. In this limit $\langle F_v\rangle$ can be written in terms of the determinant (Det) of the force-constant matrix (see e.g., Ref. 6) and the following expression can be derived:

$$\langle F_v[T,\Omega,\{c(\mathbf{R})\}]\rangle \approx \frac{1}{2}\,k_B T\sum_{\mathbf{k}} \ln\{M_A^{-3c}M_B^{-3(1-c)}\mathrm{Det}[\hbar^2\phi(\mathbf{k})/k_B^2T^2]\}, \quad (7)$$

where M_A and M_B denote the atomic masses of A and B, respectively.

By combining Eqs. (6) and (7), it is straightforward to derive the following MF expression for the Gibbs free energy:

$$\frac{1}{N}\,G_{\mathrm{MF}}(N,c,T,P) = \frac{1}{N}\,E_0 + \frac{1}{2N}\,c(1-c)\sum_{\mathbf{k}\neq 0} V(\mathbf{k}) + k_BT[c\,\ln c + (1-c)\ln(1-c)] + \frac{1}{2N}\,k_BT\sum_{\mathbf{k}} \ln\{M_A^{-3c}M_B^{-3(1-c)}\mathrm{Det}[\hbar^2\phi(\mathbf{k})/k_B^2T^2]\} + P\Omega. \quad (8)$$

In deriving Eq. (8) we have made use of the MF relations $\langle \delta c(\mathbf{k}) \delta c^*(\mathbf{k}) \rangle = Nc(1-c)$ and $S_c = -Nk_B[c \ln(c) + (1-c)\ln(1-c)]$.

Even though correlations are explicitly neglected in MF theory, it is possible to determine values of PCF's consistent with Eq. (8) using the MF theory of concentration fluctuations originally applied to alloy solid solutions by Krivoglaz[20] and Clapp and Moss[21] (KCM). When our MF free-energy function (8) is used to derive the KCM expression for the Fourier-transformed PCF, we obtain the expression

$$\langle \delta c(\mathbf{k}) \delta c^*(\mathbf{k}) \rangle = \frac{Nc(1-c)}{1 + c(1-c)[V(\mathbf{k}) - V(\mathbf{R}=0)]/k_B T}, \tag{9}$$

where $V(\mathbf{R}=0)$ is equivalent to the Brillouin-zone average of $V(\mathbf{k})$.

The MF approximation discussed in the previous paragraph is known to give rise to significant errors when applied to the calculation of c-T phase diagrams for alloy systems with energetics described by Ising and lattice-gas Hamiltonians with short-ranged interactions (see, e.g., Ref. 1). Additionally, it has been shown that in a few cases the KCM formula can lead to incorrect predictions of the location of the maximum for the PCF in reciprocal space.[22] For the purpose of assessing the accuracy of the MF approximation in the present work, we have also performed calculations of phase diagrams and PCF's using MC simulations.[12]

MC simulations were performed in the grand-canonical ensemble using periodic boundary conditions with cells containing 2000, 16 000, and 54 000 atoms. The larger sized (16 000 and 54 000) cells were required to avoid significant finite-size effects for values of the chemical field and temperature near critical points. Equilibration and sampling stages of the MC simulations were performed for 5000 and 10 000 MC steps, respectively. Enthalpy and PCF values were obtained directly from the results of the MC simulations. Phase boundaries were calculated using values of free energies derived from a thermodynamic integration technique described by de Gironcolli *et al.* in Ref. 9.

The Hamiltonian used in the MC simulations consisted of the first two terms in Eq. (3) including real-space EPI's within the range of the eighth-nearest-neighbor pair: simulations were performed both with and without the inclusion of the vibrational free-energy expression given by Eq. (7). The terms E_0, $V(\mathbf{R})$, and F_v in the MC Hamiltonian are volume- and concentration-dependent quantities. For a given temperature and concentration, the volume was assumed to be that which minimized the sum of $E_0 + F_v$ (in simulations where vibrational contributions were neglected, the volume was assumed to be that which minimized E_0). The corrections to the volume due to short-range order were therefore neglected in our study; these corrections were found to adjust the volume by an amount approximately equal to only 0.1% for the systems considered in this study. The composition dependence of the MC Hamiltonian was treated by fitting calculated values of E_0, F_v, and $V(\mathbf{R})$ to polynomials in the concentration.

C. Implementation within the embedded atom method

The SOE approach outlined in the previous subsections can be coupled with any technique which allows one to calculate the terms E_0, θ, ϕ, and ψ in Eq. (1). For example, in the work listed in Ref. 9 de Gironcolli *et al.* and Marzari *et al.* used the virtual crystal approximation, combined with linear response and pseudopotential theories in order to calculate these terms from first principles. Additionally, de Fontaine[1] has reviewed how the SOE energy can be formulated within the framework of pseudopotential-based pair potentials. In the present work we use the EAM to calculate the relevant terms arising in the SOE approach.

In the EAM, the cohesive energy of a binary alloy can be written as

$$E = \sum_{\mathbf{R}} \{c(\mathbf{R}) F_A(\rho_{\mathbf{R}}) + [1-c(\mathbf{R})] F_B(\rho_{\mathbf{R}})\} + \frac{1}{2} \sum_{\mathbf{R},\mathbf{R}'}^{\mathbf{R} \neq \mathbf{R}'} (c(\mathbf{R}) c(\mathbf{R}') U_{AA}(\Delta_{\mathbf{R},\mathbf{R}'}) + [1-c(\mathbf{R})][1-c(\mathbf{R}')] U_{BB}(\Delta_{\mathbf{R},\mathbf{R}'})$$
$$+ \{c(\mathbf{R})[1-c(\mathbf{R}')] + c(\mathbf{R}')[1-c(\mathbf{R})]\} U_{AB}(\Delta_{\mathbf{R},\mathbf{R}'})), \tag{10}$$

where F_A and F_B are the embedding functions[10,11] corresponding to A and B atoms, respectively, and U_{AA}, U_{BB}, and U_{AB} are pair interactions[10,11] appropriate for each possible type of pair in a binary alloy. In Eq. (10), $\Delta_{\mathbf{R},\mathbf{R}'}$ specifies the distance between atoms: $\Delta_{\mathbf{R},\mathbf{R}'} \equiv |\mathbf{R} + \mathbf{u}(\mathbf{R}) - \mathbf{R}' - \mathbf{u}(\mathbf{R}')|$. The variable $\rho_{\mathbf{R}}$ denotes the electron density at the location of the atom associated with site $\mathbf{R}$ due to all other atoms in the alloy. In the EAM, the electron density is approximated by a superposition of atomic densities, and for a binary alloy we have

$$\rho_{\mathbf{R}} = \sum_{\mathbf{R}'(\neq \mathbf{R})} [c(\mathbf{R}') \rho_A(\Delta_{\mathbf{R},\mathbf{R}'}) + [1-c(\mathbf{R}')] \rho_B(\Delta_{\mathbf{R},\mathbf{R}'})], \tag{11}$$

where $\rho_A(\Delta_{\mathbf{R},\mathbf{R}'})$ is the contribution to the density at $\mathbf{R} + \mathbf{u}(\mathbf{R})$ arising from an A atom located at $\mathbf{R}' + \mathbf{u}(\mathbf{R}')$ and similarly for $\rho_B(\Delta_{\mathbf{R},\mathbf{R}'})$.[10,11]

The term E_0 in Eq. (1) can be determined from Eqs. (10) and (11) by setting $c(\mathbf{R}) = c$ and $\mathbf{u}(\mathbf{R}) = 0$ for each site $\mathbf{R}$. Expressions for the terms $\theta(\mathbf{R} - \mathbf{R}')$, $\psi_\alpha(\mathbf{R} - \mathbf{R}')$, and $\phi_{\alpha,\beta}(\mathbf{R} - \mathbf{R}')$ can be derived in a straightforward manner from the partial derivatives of Eqs. (10) and (11) with respect to occupation and displacement variables. Explicitly, θ and ψ have the forms

$$\theta(R_{ij}) = [2\Delta F'(\bar{\rho}) \Delta\rho(R_{ij}) + \Delta U(R_{ij})](1 - \delta_{ij}) + \sum_{k(\neq i,j)} \hat{F}''(\bar{\rho}) \Delta\rho(R_{ik}) \Delta\rho(R_{jk}) \tag{12}$$

and

$$\psi(R_{ij})=\hat{\mathbf{r}}_{ji}[\Delta U'(R_{ij})+\hat{\rho}'(R_{ij})\Delta F'(\bar{\rho})+\Delta\rho'(R_{ij})\hat{F}'(\bar{\rho})]+\sum_{k(\neq i,j)}[\hat{\mathbf{r}}_{jk}\hat{F}''(\bar{\rho})\hat{\rho}'(R_{kj})\Delta\rho(R_{ki})], \tag{13}$$

where $R_{ij}=|\mathbf{R}_i-\mathbf{R}_j|$, $\hat{\mathbf{r}}_{ij}=(\mathbf{R}_i-\mathbf{R}_j)/R_{ij}$, and primes denote differentiation with respect to the argument. In Eqs. (12) and (13), θ and ψ are defined in terms of the derivatives of the following linear combinations of embedding functions, atomic electron densities, and pair interactions:

$$\Delta F(\rho)\equiv F_A(\rho)-F_B(\rho),\quad \hat{F}(\rho)\equiv cF_A(\rho)+(1-c)F_B(\rho),$$

$$\hat{\rho}(R_{ij})\equiv c\rho_A(R_{ij})+(1-c)\rho_B(R_{ij}),\quad \Delta\rho(R_{ij})\equiv\rho_A(R_{ij})-\rho_B(R_{ij}),\quad \bar{\rho}\equiv\sum_{j(\neq i)}\hat{\rho}(R_{ij}),$$

$$\Delta U(R_{ij})\equiv cU_{AA}(R_{ij})+(1-2c)U_{AB}(R_{ij})-(1-c)U_{BB}(R_{ij}). \tag{14}$$

The expression for the force-constant matrix (ϕ) used in the present study can be obtained from the formulas given in Ref. 11 for elemental solids, provided $\bar{\rho}$ and $\hat{F}$ are substituted for the elemental electron charge densities and embedding functions, respectively, and provided the pair interaction is replaced by the average $U(R_{ij})\equiv c^2U_{AA}(R_{ij})+(1-c)^2U_{BB}(R_{ij})+2c(1-c)U_{AB}(R_{ij})$.

The EAM potentials for Cu-Ni and Cu-Ag used in the present study have been derived, according to the procedure discussed by Foiles,[23] by fitting to elemental equilibrium lattice constants, sublimation energies, elastic constants, vacancy formation energies, and dilute heats of solution. Even though the only alloy information used in the fitting was heats of solution for dilute compositions, we found that the energetics of concentrated Cu-Ni and Cu-Ag alloys were well described by these potentials. Specifically, predicted heats of mixing agreed well with experimental measurements[24] at all compositions for Cu-Ni alloys (see below). Also, formation energies calculated by the EAM for (hypothetical) ordered Cu-Ag compounds were found to agree to within 7 meV/atom with the values computed from first principles by Wei *et al.*[25] For Au-Ni, we found that potentials derived by fitting only to properties of the elemental solids and dilute alloys underestimated considerably the heats of mixing measured experimentally[24] for concentrated compositions. Therefore, information about the energetics of concentrated alloys was included in the fitting of the Au-Ni potentials used in the present study. Specifically, included in the fitting of these potentials were the first-principles-calculated values of the formation energies for five Au-Ni compounds (with unrelaxed $L1_2$, $L1_0$, "40," and $Z2$ structures) computed by Lu and Zunger.[26]

D. Comparison with other approaches

The combined EAM-SOE-MF approach outlined in this section is similar in some ways to another technique which has been applied to the study of substitutionally disordered alloys within the context of the EAM. This technique is referred to as the free-energy minimization method (FEMM), and it is described in detail in a recent paper by Najafabadi *et al.*[27] For homogeneous solid-solution phases, there are three main differences between the FEMM and SOE-MF approaches: (1) The FEMM description of alloy energetics reduces to our E_0 term in Eq. (3); consequently, the contribution of the chemical interaction term (θ) to the energy is neglected in the FEMM. (2) Equilibrium displacements for homogeneous solid solutions (with high-symmetry structures such as fcc and bcc) are zero by symmetry in the FEMM. Consequently, the relaxation-energy contribution to the alloy enthalpy is neglected in the FEMM. (3) The local harmonic model[28] is used to calculate vibrational free energies in the FEMM; in our approach, use is made of the high-temperature limit of an approximate quasiharmonic treatment for vibrations. In order to gauge the relative accuracies of the FEMM and SOE-MF approaches, we performed a comparison of the values of calculated thermodynamic properties for *unrelaxed* Cu-Ag solid solutions. Excellent agreement (within 1 meV/atom) was found between our SOE-EAM results and those obtained with the FEMM (Refs. 29 and 30) for both heats of mixing and Gibbs free energies of formation. For applications to *homogeneous* solid solutions, the SOE approach offers the following advantages over the FEMM: It provides (1) a method for including the contributions of relaxation energies (associated with static local atomic displacements) to calculated values of alloy thermodynamic properties and (2) a convenient framework for analyzing SRO and average bond distances in disordered solid-solution phases. In the case of *inhomogeneous* solid solutions (e.g., solid solutions with extended defects), the FEMM is more versatile in general since, in contrast to the SOE method, it is not formally based on the notion of an underlying reference parent-lattice structure.

The SOE approach discussed in this section shares many features in common with the concentration-wave (CW) method, the generalized perubation method (GPM), and the embedded cluster method (ECM) (each of these methods are described in detail in Refs. 6–8). In particular, these methods are also based upon perturbations of a random substitutional alloy at a specific composition of interest. In contrast to the SOE methods outlined in this section and in Refs. 1 and 9, in the CW, GPM, and CWM approaches the energetics (and the electronic structure) of the random alloy is approximated via the (single-site) coherent-potential-approximation[31] (CPA). The CPA-based methods as yet have not been used to treat displacive effects in substitutional alloys. However, generali-

zations of the CW method for treating displacements have been outlined along the lines of the second-order formalism discussed in Sec. II A.[7,32]

A variety of approaches based upon the cluster expansion formalism (for a review, see Ref. 3) have been applied widely to the calculation of structural and thermodynamic properties of substitutional alloys, including the effects of atomic displacements. Within the cluster-expansion formalism, relaxation effects in disordered alloys have been accounted for in a number of ways.[3,5,13,15,16,25,33–36] In one type of approach, effective volumes and elastic moduli are assigned to each type of atomic arrangement associated with a point[13,33] or multiatom[25,34,36] cluster. Sanchez *et al.* have also generalized this type of theory in order to calculate vibrational properties of disordered alloys within a Debye-model formalism.[13] The various parameters which enter into the effective-volume cluster-expansion theories are commonly derived from the results of first-principles total-energy calculations for ordered alloy structures with high-symmetry crystal structures. In alternative cluster-expansion approaches,[5,35] relaxation effects are incorporated into the values of effective cluster-interaction (ECI) parameters directly. The values of the ECI's, including the contributions of the relaxation energy, are obtained in these methods by fitting to first-principles-calculated total energies for a large set of ordered structures (including structures with low symmetries and many structural degrees of freedom) which have been relaxed with respect to all cell-internal and external structural degrees of freedom.[5]

In the cluster-expansion approaches, relaxation energies and chemical interactions are parametrized by pair as well as higher-order multiple-atom ECI's, in contrast to the SOE method in which relaxation and ordering energies are described by effective *pair* interactions only. While third- and higher-order displacive effects are automically built into the fitted values of the ECI's in the cluster expansion approaches, the consideration of such terms within the formalism outlined in Sec. II A would require going beyond second-order terms in the expansion given by Eq. (1). The SOE approach offers the distinct advantage that it allows the magnitudes of the atomic displacements in substitutionally disordered alloys to be calculated directly; this is not generally possible in the current implementation of the cluster-expansion approaches. In the following section the results of the present SOE-based calculations will be compared with those of previous studies performed using cluster-expansion methods.

III. RESULTS

A. Accuracy of the SOE approach

In order to assess the accuracy of the approach for treating alloy energetics described in the previous section, we performed several tests comparing results obtained (using the same set of EAM potentials) from direct calculations and from the approximate SOE method. The first test involved the zero-temperature cohesive energies of ordered alloy compounds having Ll_2 and Ll_0 structures. The direct calculations were performed by evaluating Eq. (10) with the values of $\{c(\mathbf{R})\}$ appropriate for each ordered structure and with the values of $\{\mathbf{u}(\mathbf{R})\}$ all set equal to zero (the c/a ratio for the tetragonal Ll_0 structure was fixed at its ideal value: $c/a=1$). The SOE cohesive energies were obtained from the first two terms in Eq. (3) using the values of $\delta c(\mathbf{k})$ obtained by a Fourier transform of the occupation variables appropriate for each structure. In both the direct and SOE calculations, the cohesive energies were minimized with respect to volume. For each of the Ll_2 and Ll_0 structures in the Cu-Ni, Au-Ni, and Cu-Ag alloy systems, we found that the SOE and direct calculations gave cohesive energies which agreed to within 3 meV/atom.

Our second test of the SOE involved the zero-temperature cohesive energies for relaxed, disordered alloys with equiatomic compositions. In this case the direct numbers were obtained by averaging the energy, calculated using Eq. (10), for ten 864-atom supercells which contained randomly generated atomic configurations. The energy of each supercell was minimized with respect to volume and also with respect to the displacements $\{\mathbf{u}(\mathbf{R})\}$, where the latter minimization was performed using the conjugate-gradient method.[37] The SOE cohesive energies for the relaxed, equiatomic, disordered alloys were obtained by minimizing the zero-temperature and zero-pressure version of Eq. (8) with respect to volume. In this test excellent agreement between the results of direct and SOE calculations was again obtained: Cohesive energies were found to agree to within 3 meV/atom for each alloy system considered.

In order to estimate the accuracy of the approximate treatment for atomic vibrations outlined above, vibrational free energies were computed both by a direct quasiharmonic method (using the EAM expressions for the dynamical matrix given by Daw *et al.* in Ref. 11) and from Eq. (7) for equiatomic Cu-Ag and Cu-Ni alloys at 600 and 900 K. Direct calculations of the quasiharmonic vibrational free energies were performed for both disordered alloys and for ordered compounds with the Ll_0 structure. Analogous to the calculations described in the previous paragraph, the direct calculations for disordered alloys were performed using 108-atom supercells and results were averaged over several randomly generated atomic configurations. For CuNi the SOE expression for the vibrational free energy gives results which are at most 3 meV/atom (2%) and 2 meV/atom (1.5%) more negative for ordered and disordered alloys, respectively, at each temperature considered. For CuAg the magnitudes of the vibrational free energies were found to be larger, as was the discrepancy between results obtained from direct and SOE calculations. Specifically, for CuAg the vibrational free energies calculated from Eq. (7) are as much as 10 meV/atom (3%) and 15 meV/atom (4%) less negative than those obtained by direct calculations for disordered and ordered alloys, respectively.

B. Heats of mixing

In Fig. 1 we present the results of EAM-SOE calculations for zero-temperature heats of mixing (ΔH) for relaxed and unrelaxed random solid solutions in fcc Cu-Ni [Fig. 1(a)], Cu-Ag [Fig. 1(b)], and Au-Ni [Fig. 1(c)] alloys. The solid lines in Fig. 1 give the heats of mixing for *relaxed* alloys which were computed as the difference in enthalpy between the random solid solution of a given composition and the concentration-weighted average of the enthalpies of the constituent elements. The enthalpies were computed by mini-

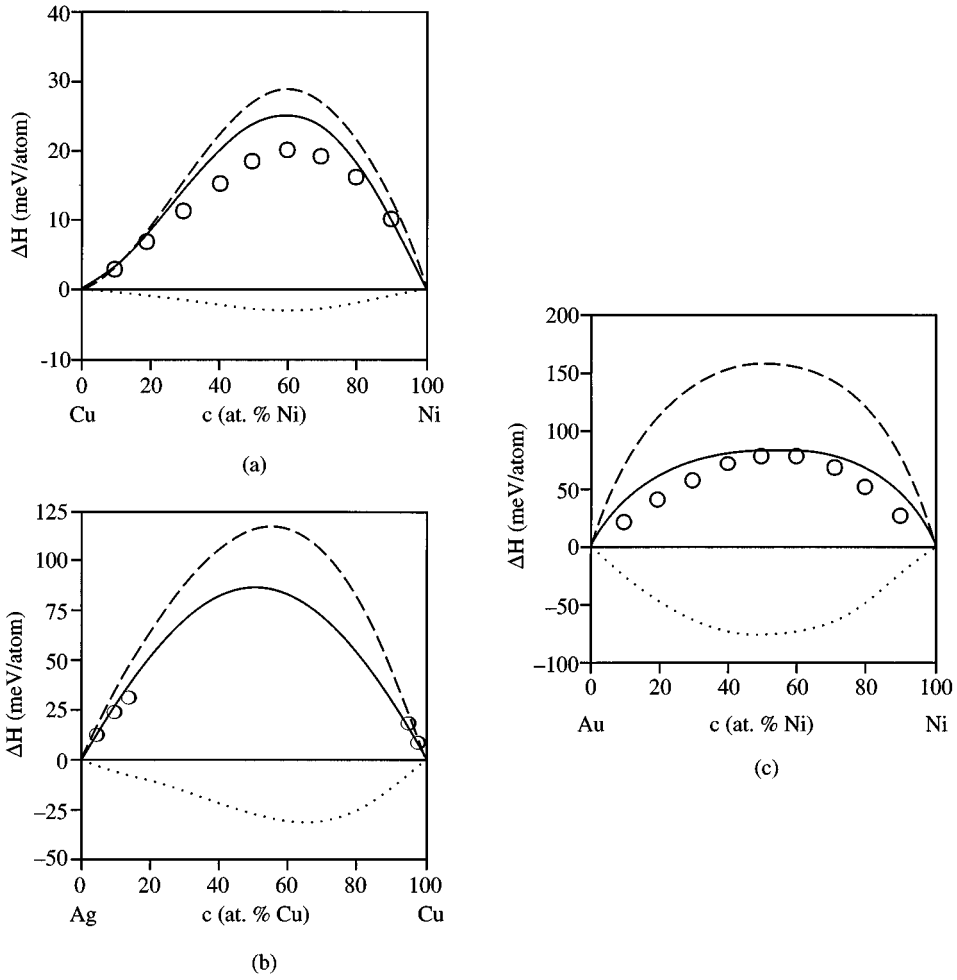

FIG. 1. Calculated and experimentally measured values of the heats of mixing (ΔH) for Cu-Ni (a), Cu-Ag (b), and Au-Ni (c) solid solutions. The solid lines indicate total calculated values of ΔH for relaxed alloys, the dashed lines correspond to values of ΔH for unrelaxed solid solutions, and the dotted lines give values of relaxation energies (see text). The open circles indicate measured values of ΔH, taken from Ref. 20, for Cu-Ni alloys at 973 K, Cu-Ag alloys at 1052 K, and Au-Ni alloys at 1150 K.

mizing Eq. (8) with respect to volume at $T=0$ K. The dashed lines in Fig. 1 correspond to the heats of mixing calculated for *unrelaxed* random alloys in which the atoms are artificially constrained to occupy the ideal positions on an fcc lattice (i.e., displacements were all set to zero); these results were computed also from Eq. (8) neglecting the relaxation-energy contribution [the second term on the right-hand side of Eq. (4)] to the EPI. The dotted lines in Fig. 1 give the values of the relaxation energies defined as the difference between the heats of mixing for relaxed and unrelaxed alloys.

The degree of size mismatch for each of the alloy systems considered in the present study can be assessed by computing the ratio $\Delta a/\bar{a}$, where Δa and $\bar{a}$ are, respectively, the difference and the average of the lattice parameters for the two constituent elements. For Cu-Ni, Cu-Ag, and Au-Ni, the values of $\Delta a/\bar{a}$ are, respectively, 2.5%, 12.5%, and 14.7%. A comparison of the dotted lines in Fig. 1 shows that a correlation exists between the magnitudes of the relaxation energies and the degree of size mismatch, as expected. In particular, for Cu-Ni the relaxation energy is smallest with a value of maximum magnitude equal to 3 meV/atom. For Cu-Ag and Au-Ni the relaxation energies are more sizable with magnitudes as large as 30 and 80 meV/atom, respectively.

The open circles in Fig. 1 symbolize the values of ΔH measured experimentally[24] at finite temperatures for Cu-Ni, Cu-Ag, and Au-Ni solid solutions. For Cu-Ni the calculated results for random alloys at zero temperature and the measured values for solid solutions containing SRO at $T=973$ K [solid line and open circles, respectively, in Fig. 1(a)] agree to within 5 meV/atom. We found that the agreement with the experimentally measured values of ΔH was improved when finite-temperature and SRO corrections were included in our calculations. Specifically, we recalculated the values of the cohesive energies for Cu-Ni solid solutions and pure elements using lattice parameters which minimized the free energy given by Eq. (8) at $T=973$ K. Additionally, in the calculations for the alloys we included SRO effects through the use of MC simulations. The effect of SRO was to *lower* the calculated heats of mixing by as much as 4 meV/atom for near-equiatomic alloys. The corrections to ΔH due to thermal expansion were found to be smaller in magnitude for Cu-Ni; their effect was to *raise* the calculated values of ΔH by a maximum value of 2 meV/atom.

TABLE I. Mean-field-calculated and experimentally measured values of critical temperatures (T_c) and critical compositions (x_c) for phase separation in the Cu-Ni, Cu-Ag, and Au-Ni alloy systems. All temperatures are in kelvin, and compositions are given in units of atomic percent. The results I, II, and III correspond to calculations performed I neglecting both relaxation energy and vibrational contributions to the alloy free energy, (II) including relaxation energy, but neglecting vibrational contributions, and (III) including both relaxation energy and vibrational free-energy contributions. Experimental results listed in the final row are taken from Ref. 28.

	Cu-Ni		Cu-Ag		Au-Ni	
Method	T_c	x_c (Ni)	T_c	x_c(Cu)	T_c	x_c (Ni)
I	1050	63	3170	63	3550	79
II	900	63	2270	49	2460	85
III	900	67				
Experiment	628	67.3			1083	70.6

The agreement between calculated and experimentally measured values of the heats of mixing for relatively dilute Cu-Ag alloys is seen in Fig. 1(b) to be excellent. This good agreement is not surprising since experimentally measured dilute heats of solution were used in the fitting of the EAM potentials for Cu-Ag. For Au-Ni alloys [Fig. 1(c)], the experimentally measured and calculated values of ΔH agree very well for near-equiatomic alloys, although significant discrepancies are found for more dilute compositions. These discrepancies cannot be attributed to finite-temperature and SRO effects neglected in the calculated values. Rather, they arise from errors associated with the EAM potentials developed for Au-Ni.

The values of the heats of mixing presented in Fig. 1 can also be compared to results of previous first-principles calculations[13,16,25,26,36,38] performed within the cluster-expansion framework using various approximations (see discussion in Sec. II D) for the treatment of atomic relaxations in the Cu-Ni, Cu-Ag, and Au-Ni alloy systems. In the case of the Cu-Ni system, the values of ΔH plotted in Fig. 1(a) are roughly 15 meV/atom larger in magnitude than those obtained by Amador and Bozzolo.[36] In agreement with our findings, Amador and Bozzolo find that SRO has a weak effect on the calculated values of ΔH for near-equiatomic Cu-Ni alloys at $T=973$ K. For dilute Cu-Ag solid solutions (containing less than 10 at. % Cu and greater than 90 at. % Cu), our results for ΔH agree to within 5 meV/atom with the ''relaxed'' values calculated by Wei *et al.*[25] Values of ΔH for more concentrated compositions in the Cu-Ag system have been calculated by Sanchez *et al.*[13] and Terakura *et al.*[38] When local relaxation effects are neglected, these authors obtain values of ΔH for the equiatomic composition equal to 140 meV/atom (Ref. 13) and 540 meV/atom (Ref. 38). The calculated values of Sanchez *et al.* are more consistent with the unrelaxed results plotted by the dashed line in Fig. 1(b). An even better level of agreement exists between our results and those of Sanchez *et al.* for the values of ΔH calculated including relaxation effects: In this case our values are smaller for the equiatomic composition by 13 meV/atom. It is interesting to note, however, that the value of the relaxation energy for CuAg obtained using an effective-volume method (see Sec. II D) by Sanchez *et al.* is roughly twice as large as that found in the present study. For Au-Ni alloys, values of the heats of mixing have been calculated including relaxation effects by Amador and Bozzolo,[36] Lu and Zunger,[26] and Colinet *et al.*[16] The best level of agreement with the results in Fig. 1(c) and with experimental measurements for concentrated alloys is found for the relaxed values calculated by Colinet *et al.* (solid line in Fig. 2 of Ref. 16): At $c=0.5$ our results for ΔH are only 5 meV/atom larger than those obtained from first-principles calculations by these authors. The values of ΔH at $c=0.5$ calculated by Lu and Zunger and by Amador and Bozzolo are roughly twice as large as those shown in Fig. 1(c). However, the magnitudes of the relaxation energy for AuNi calculated by these authors agree well (within 9 meV/atom) with the value of 77 meV/atom found in this study.

C. Finite-temperature phase stability

Table I and Fig. 2 display experimentally measured[39] and calculated results pertaining to the thermodynamic stability of Cu-Ni, Cu-Ag, and Au-Ni solid solutions. The computed results were obtained from MF calculations and MC simulations according to the methods outlined in Sec. II B. In Table I values of the critical temperatures (T_c) and critical compositions (x_c) for solid-state phase separation are listed. The computed values are the results of MF calculations which were performed using the following three levels of approximation: (I) neglecting both relaxation-energy and vibrational contributions to the free energy, (II) including relaxation-energy contributions but neglecting vibrational contributions, and (III) including both relaxation-energy and vibrational contributions. In Fig. 2, MF- and MC-calculated phase diagrams are plotted for Cu-Ni and Cu-Ag alloys. The dashed and solid lines in Fig. 2 correspond to MF- and MC-calculated phase boundaries, respectively. In the case of Cu-Ni [Fig. 2(a)], these phase boundaries were computed including both vibrational and relaxation-energy contributions to the alloy free energy. For Cu-Ag, relaxation-energy, but not vibrational, free-energy contributions were considered in the calculations of the phase diagrams shown in Fig. 2(b).

From a comparison of the MF-calculated results listed in the rows labeled I and II in Table I, it can be seen that the relaxation energy is responsible for a lowering of the calculated values of T_c by 14% (150 K), 28% (900 K), and 31% (1090 K) for Cu-Ni, Cu-Ag, and Au-Ni alloys, respectively.

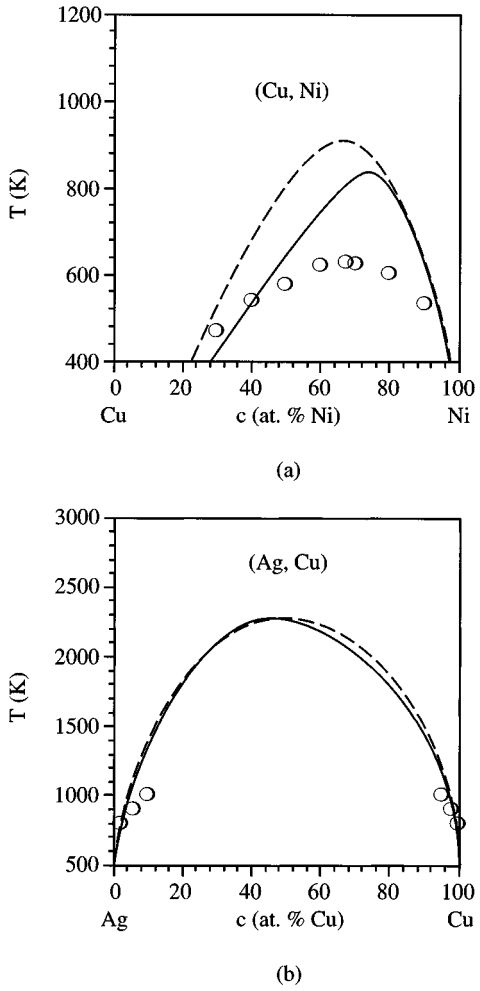

FIG. 2. Calculated and experimentally measured solid-state portions of the composition-temperature phase diagrams for Cu-Ni (a) and Cu-Ag (b). Dashed and solid lines were calculated using the mean-field approximation and Monte Carlo simulations, respectively. In the calculations for Cu-Ni, both vibrational and relaxation-energy contributions to the alloy free energy were included; for Cu-Ag, relaxation-energy but not vibrational free-energy contributions were considered. The open circles were taken from the experimentally measured phase diagrams compiled in Ref. 28.

Additionally, relaxation energies change the values of x_c for Cu-Ag and Au-Ni solid solutions by 14 and 6 at. %, respectively. In the work of Sanchez *et al.*[13] for Cu-Ag the effect on the calculated value of T_c due to the relaxation energy was estimated to be nearly twice as large (50%, 1700 K) as that found in this study; this result is consistent with the fact that the relaxation energy in Ref. 13 was found to be roughly twice as large as ours for concentrated alloys. Sanchez *et al.* found that the calculated value of x_c changed from roughly 65 to 50 at. % Cu when the relaxation-energy contribution to the free energy was included in the calculation of the Cu-Ag phase diagram; these results are in excellent agreement with the values of x_c listed in rows I and II of Table I. Wei *et al.*[25] also estimated the effects which (local) relaxation energies have on the calculated Cu-Ag phase diagram, and their results are in nearly perfect agreement with those of Sanchez *et al.* concerning the effect on the calculated values of T_c. However, Wei *et al.* estimated that the relaxation energy has almost no effect on the calculated value of the critical composition (x_c), contrary to the findings of both this study and that of Sanchez *et al.*

For Cu-Ni the results listed in the rows labeled II and III in Table I indicate that the main effect of the vibrational free energy is to shift the calculated value of x_c to a more Ni-rich composition. For Cu-Ag and Au-Ni, calculated values of T_c and x_c could not be obtained including vibrational contributions to the free energy since, with the sets of EAM potentials used in the present study, both of these alloys are predicted to be dynamically unstable at temperatures lower than T_c.[40] For Cu-Ag alloys at 1000 K, we found that vibrational contributions to the free energy are responsible for an approximately 3 at. % increase in the calculated solubility limits for both Cu- and Ag-rich compositions. A qualitatively similar effect of the vibrational free-energy contributions on the solubility limits in Cu-Ag was found by Sanchez *et al.*[13]

An assessment of the magnitudes of the errors associated with the MF approximation in the present study can be obtained from a comparison of the dashed and solid lines plotted in Fig. 2. In the case of Cu-Ni, Fig. 2(a), MF and MC results agree well for Ni-rich compositions, although significant discrepancies are found near equiatomic compositions. Specifically, near the composition 45 at. % Ni, phase boundaries obtained from MC simulations are lower than those derived from MF calculations by approximately 20% (160 K). For Cu-Ag, MF- and MC-calculated phase transition temperatures are found to be in better agreement; a maximum difference of only 3% is found in the calculated phase transition temperatures near 70 at. % Cu.

Results listed in the last row of Table I and shown as open circles in Fig. 2 are taken from experimentally measured phase diagrams.[39] In Fig. 2(a) it can be seen that our calculations reproduce qualitatively the asymmetry in the miscibility gap for Cu-Ni. Our most accurate calculated value of T_c for Cu-Ni, obtained from MC simulations including both relaxation and vibrational contributions to the free energy, is higher than the experimentally measured value by 230 K. This overestimation of the value of T_c for Cu-Ni is consistent with the fact that the EAM-SOE-computed heats of mixing shown in Fig. 1(a) are slightly larger in magnitude than the values obtained from calorimetry experiments.[24] For Cu-Ag alloys, below the eutectic temperature of 1053 K, the calculated phase boundaries underestimate only slightly the experimentally measured solubility limits shown in Fig. 2(b) for Cu-rich compositions. On the Ag-rich side of the phase diagram, the discrepancy between the calculated and experimentally measured phase boundaries is slightly more significant. As alluded to above, when vibrational free-energy contributions are included in the calculation of the miscibility-gap phase boundaries for Cu-Ag at temperatures below the eutectic, the computed solubility limits increase and the agreement with experimental measurements is improved for both Cu- and Ag-rich compositions. According to the results for Au-Ni listed in Table I, the MF-SOE-EAM calculation, which included relaxation-energy contributions to the free energy, resulted in a computed T_c which significantly overestimates the measured value. The reason for this poor level of agreement between calculated and measured values of T_c for Au-Ni can be attributed largely to the failure of the EAM

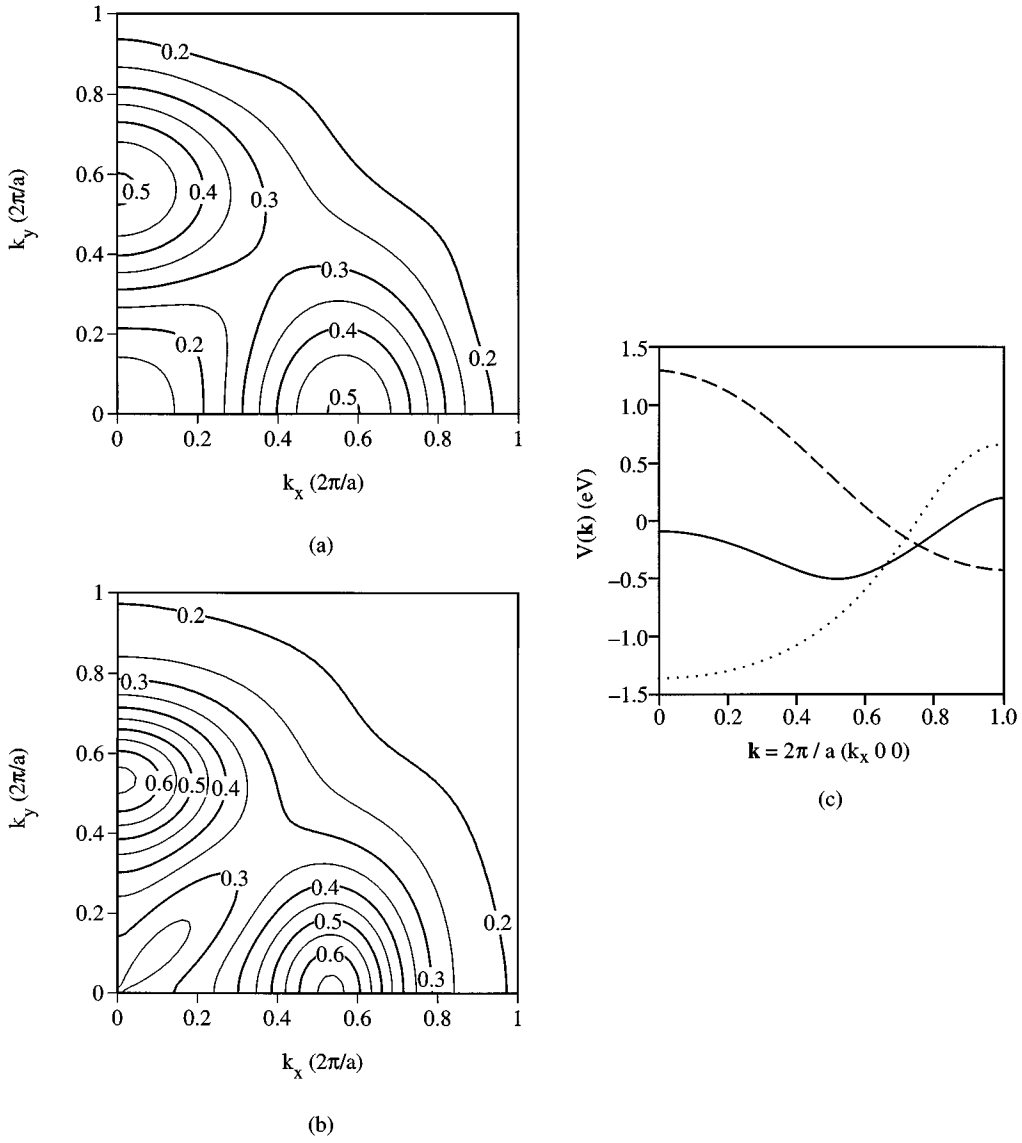

FIG. 3. Calculated Fourier-transformed (FT) pair-correlation functions (PCF's) and effective pair interactions (EPI's) for a Au−40 at. % Ni alloy. FT PCF's, calculated using Monte Carlo simulations (a) and the mean-field approximation (b), are plotted in the (001), $k_z=0$, plane of reciprocal space. The FT EPI is plotted with a solid line in (c) between the Γ ($\langle 000\rangle$) and X ($\langle 100\rangle$) points. The dashed and dotted lines in (c) give the ''chemical'' and relaxation-energy contributions (see text) to the FT EPI, respectively.

potentials to accurately reproduce the curvature associated with the composition dependence of the heats of mixing plotted in Fig. 1(c).

D. Short-range order and effective pair interactions

The SRO of Au-Ni solid solutions has been studied experimentally by a number of investigators (see Refs. 41 and 42 as well as references listed therein) using diffuse scattering methods. Results obtained by Wu and Cohen[41] show that the Fourier-transformed (FT) PCF for a Au−40 at. % Ni alloy has a maximum value away from the high-symmetry special points[1,4,6] in the fcc Brillouin zone. Specifically, the PCF is found to peak near $\mathbf{k}=\langle 0.6,0,0\rangle$. In the current study we computed the Fourier-transformed PCF for a Au−40 at. % Ni alloy at a temperature of 2300 K (which is just above the calculated miscibility-gap phase boundary at this composition) using both MF calculations and MC simulations. In the MF calculations the FT PCF was determined directly using Eq. (9). MC simulations were used to compute values of the real-space PCF's for the first eight nearest-neighbor shells; these results were then Fourier transformed in order to compare with experimental measurements and MF calculations.

The results of the MC simulations and MF calculations for the FT PCF's are plotted in the {001} plane of reciprocal space in Figs. 3(a) and 3(b), respectively. The features displayed in each of these figures are seen to be qualitatively very similar. In particular, in excellent agreement with experimental measurements,[41] both the MC- and MF-calculated PCF's take on maximal values at positions between the Γ ($\langle 0,0,0\rangle$) and X ($\langle 1,0,0\rangle$) points of the fcc Brillouin zone. Specifically, the MC and MF results display PCF peaks at approximately $\mathbf{k}=\langle 0.55,0,0\rangle$ and $\mathbf{k}=\langle 0.5,0,0\rangle$, respectively. The maximal value of the FT PCF calculated by

MC simulations is lower than that obtained from MF theory [Eq. (9)]; the origin of this discrepancy is likely due to the fact that the critical temperature obtained by MC simulations is lower than that derived from MF. Additionally, the MF results [Fig. 3(b)] show structure near the origin which is absent in Fig. 3(a). The reason this structure is not present in the latter figure stems from the fact that the MC-calculated FT PCF's were obtained from the values of the real-space PCF's corresponding to only the first eight nearest-neighbor shells; from an analysis of the MF results, it was found that the values of PCF's corresponding to pairs spanning distances greater than the eighth neighbor are needed to reproduce the structure shown in Fig. 3(b) near the Γ point.

An understanding of the possible origin of the unusual SRO observed in Au-Ni solid solutions can be obtained from an analysis of the calculated EPI shown in Fig. 3(c). In this figure the solid line gives the value $\Delta V(\mathbf{k})=V(\mathbf{k})-V\ (\mathbf{R}=0)$ [see Eq. (9)] calculated for a Au−40 at. % Ni alloy as a function of $\mathbf{k}$ along the line joining the Γ and X points. From Eq. (9) it can be seen that, within the MF theory of concentration fluctuations, the PCF has a maximal value at $\mathbf{k}$ points corresponding to global minima for the function $V(\mathbf{k})$. In agreement with Fig. 3(b), the quantity $\Delta V(\mathbf{k})$ is seen to have a minimum value at $\mathbf{k}\approx\langle 0.5,0,0\rangle$. In Fig. 3(c) the dashed and dotted lines indicate the ''chemical'' and relaxation-energy contributions to $\Delta V(\mathbf{k})$ defined as $\theta(\mathbf{k})-\theta(\mathbf{R}=0)$ and $P(\mathbf{k})-P(\mathbf{R}=0)$, respectively, where $P(\mathbf{k})=-\psi(\mathbf{k})\phi^{-1}(\mathbf{k})\psi^{*}(\mathbf{k})$. The chemical contribution to $\Delta V(\mathbf{k})$ (dashed line) is seen to have a minimum value at the X point. Therefore, chemical interactions give rise to a tendency for ordering SRO of the type consistent with Ll_2 and Ll_0 structures. By contrast, the relaxation-energy contribution to $\Delta V(\mathbf{k})$ (dotted line) has a minimal value at the Γ point, indicating a preference for SRO of clustering type. Therefore, we find that for Au−40 at. % Ni alloys, the minimum of $V(\mathbf{k})$ and the corresponding peak in the PCF for values of $\mathbf{k}$ between the Γ and X points arise as a consequence of a competition between chemical and relaxation-energy contributions to the EPI, which, respectively, favor SRO of ordering and clustering types.

SRO in the Au-Ni system has been the subject of several theoretical studies in the past.[26,43,44] In the recent work of Lu and Zunger,[26] the properties of Au-Ni solid solutions were studied using a first-principles, cluster-expansion-based method. By combining this approach with MC simulations, Lu and Zunger calculate SRO for a Au−40 at. % Ni solid solution which is also in good agreement with experimental measurements: They find a peak in the SRO in reciprocal space between the Γ and X points at approximately $\langle 0.8,0,0\rangle$. Therefore, the experimentally observed position for the peak in the SRO in reciprocal space (at roughly $\langle 0.6,0,0\rangle$) is bracketed by the peak positions obtained in the present calculations and in Ref. 26. Lu and Zunger note that their calculated value of the nearest-neighbor Warren-Cowley SRO parameter (-0.074) is opposite in sign compared to the value measured experimentally by Wu and Cohen (0.039),[41] although it agrees fairly well with an estimate (-0.030) obtained from earlier experiments on polycrystalline samples performed by Flinn *et al.*[42] Our computed values for the nearest-neighbor SRO parameter are 0.034 and 0.052, obtained from MC simulations and MF calculations, respectively; our results therefore agree best with the measurements of Wu and Cohen.[41]

In Fig. 3(c) it is shown that the chemical and relaxation-energy contributions to the Fourier-transformed EPI are comparable in magnitude for the Au-Ni system. The magnitudes of the relaxation-energy contributions to EPI's can be analyzed further from the results plotted in Fig. 4. In Figs. 4(a), 4(b), and 4(c), calculated values of EPI's are plotted as a function of the neighbor shell in real space for equiatomic Cu-Ni, Cu-Ag, and Au-Ni solid solutions, respectively. Each white bar indicates a value of $\theta(\mathbf{R})$, corresponding to the chemical contribution to the EPI. For each alloy system, the chemical EPI's are seen to decay rapidly as a function of distance. Specifically, the nearest-neighbor values are found to dominate and $\theta(\mathbf{R})$ is negligible beyond the fourth-neighbor-pair distance in all cases. The solid black bars in Fig. 4 indicate values of the EPI's including both chemical and relaxation-energy [$P(\mathbf{R})$] contributions. A comparison of the black and white bars in Fig. 4(a) shows that for CuNi the contributions from $P(\mathbf{R})$ are relatively small. For CuAg and AuNi the situation is quite different. Specifically, the relaxation energy is found to change the sign of the first- and second-neighbor pair interactions for CuAg, as well as the nearest-neighbor EPI for AuNi. Additionally, $P(\mathbf{R})$ gives rise to EPI's which decay slowly in real space. The fact that sizable relaxation energies lead to long-ranged EPI's has been noted also in previous semiempirical[1] and first-principles[5,35] studies.

E. Local atomic displacements: Average nearest-neighbor bond lengths

In the previous three subsections, we analyzed the effects which local atomic displacements have on the SRO and thermodynamic properties of solid solutions. In this subsection we consider the nature of the local atomic displacements themselves. Specifically, in Fig. 5 we show calculated and experimentally measured[41,45] values of average nearest-neighbor (NN) bond lengths (R) for Au-Au [Fig. 5(a)], Au-Ni [Fig. 5(b)], and Ni-Ni [Fig. 5(c)] pairs as a function of alloy composition for Au-Ni solid solutions. The calculated values, shown as solid circles in Fig. 5, were obtained for random alloys (i.e., neglecting SRO) using Eqs. (2) and (5). The experimental values plotted with open circles were obtained from extended x-ray-absorption fine-structure (EXAFS) measurements performed by Renaud *et al.*[45] The open squares give NN bond lengths for Au−40 at. % Ni alloys derived from the magnitudes of the average displacements obtained by Wu and Cohen[41] from an analysis of their diffuse scattering data. The dashed lines in Fig. 5 correspond to ''Vegard's law'' values of R which have been calculated assuming no displacements and a linear dependence of lattice parameter on composition.

Both calculated and experimentally measured results plotted in Figs. 5(a) and 5(c) show that the lengths of the NN Au-Au and Ni-Ni bonds are greater and smaller, respectively, than the average values given by Vegard's law, as expected. From an analysis of Figs. 5(a) and 5(c), it can be seen that the displacements with the largest magnitudes (i.e., the largest deviations from Vegard's law) are found for like NN bonds between minority species in dilute alloys. For the

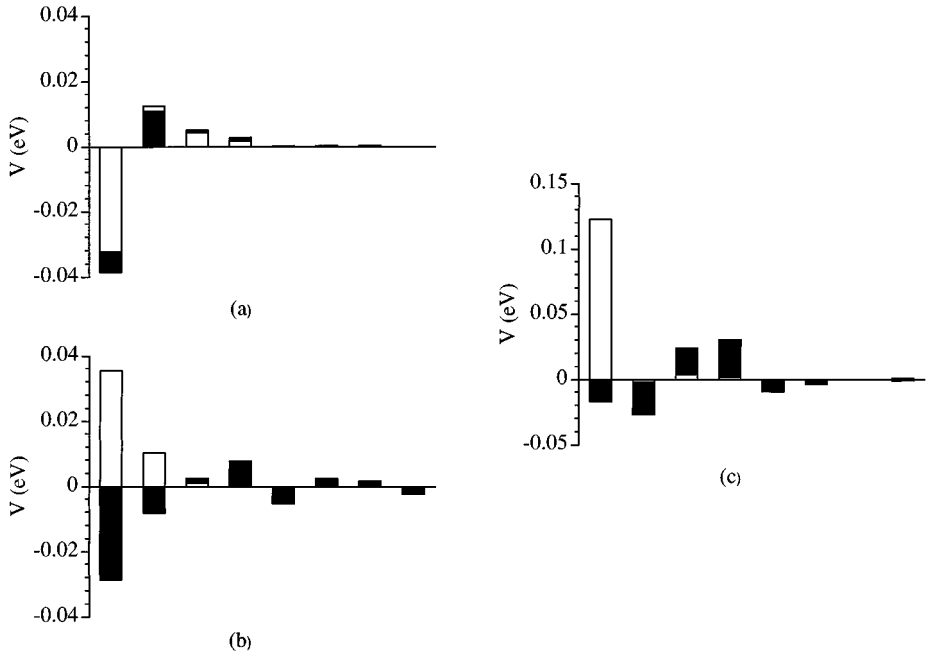

FIG. 4. Calculated values of the effective pair interactions (V) for equiatomic Cu-Ni (a), Cu-Ag (b), and Au-Ni (c) alloys. The horizontal axis represents neighbor shells; results for shells ranging from the first to the eighth neighbor are plotted from left to right in each figure. The white bars give values of the ''chemical'' contribution θ [see Eq. (1)] to the effective pair interaction. The solid black bars give the total values of the effective pair interactions, including both chemical and relaxation-energy contributions (see text).

mixed Au-Ni bonds, both the EXAFS data and the calculated results indicate that the values of the displacements change sign as a function of composition: For Ni- and Au-rich compositions, respectively, the Au-Ni bond lengths deviate positively and negatively from Vegard's law.

In the case of Au-Au NN bonds, the agreement between the different experimental data and the calculated results for R is quite good, although computed bond lengths are consistently slightly larger than the measured values. For Au-Ni bonds at 40 at. % Ni, there is a significant difference between the values of R obtained from the two different experimental methods. In this case our calculations are in very good agreement with the EXAFS results. By contrast, for Ni-Ni bonds our computed bond lengths differ greatly from the values obtained by EXAFS measurements for Au-rich compositions, and better agreement is found with the diffuse scattering data at 40 at. % Ni. A comparison of the data plotted with open circles in Figs. 5(b) and 5(c) shows that the EXAFS results predict that Ni-Ni and Au-Ni bond lengths are roughly equal for Au-rich compositions. This surprising result is not reproduced by either our calculations or those of Amador and de Fontaine,[46] and it warrants further experimental and theoretical investigation in our opinion.

IV. SUMMARY AND DISCUSSION

A. SOE approach

In the second section of this paper, a SOE approach was outlined for the purpose of studying the structural and thermodynamic properties of alloy solid solutions. This approach can in principle be coupled with any technique which allows one to calculate the E_0 term as well as the various second-order derivatives arising in Eq. (1). For the purposes of the present study, we described the details of how the SOE method can be implemented within the framework of the EAM in Sec. II C.

When combined with MF statistical-mechanical calculations, the SOE approach provides a highly efficient technique for computing both structural and thermodynamic properties of alloy solid solutions. In order to estimate the magnitudes of the errors associated with the various approximations used to formulate the MF-SOE approach, a number of numerical tests was performed comparing predictions of this method with those of more accurate calculations. The results discussed in Sec. III A demonstrate that the SOE expression for the alloy energy is accurate to within a few meV/atom. This excellent level of accuracy is achieved both for ordered compounds and relaxed disordered solid solutions even though the SOE is formulated with respect to a homogeneous disordered reference state with no displacements.

In Sec. II B we described a method which allows alloy vibrational free energies to be calculated within the SOE framework. For elemental solids this approach reduces to the high-temperature limit of the quasiharmonic theory. For alloys the approach is approximate even within the high-temperature–quasiharmonic framework due to the neglect of higher-order terms in the expansion, Eq. (1), of the alloy energy.[47] In Sec. III A we discussed results which demonstrate that the approximate SOE method reproduces values of F_v from direct quasiharmonic calculations for ordered and disordered alloys to within a few percent. A problem associated with the SOE treatment of vibrational free energies is that it leads to an expression for F_v which is independent of the alloy configuration at a given concentration. This shortcoming can be remedied and the accuracy of the approach can be improved through the consideration of third-order terms in the expansion of the alloy energy.[47]

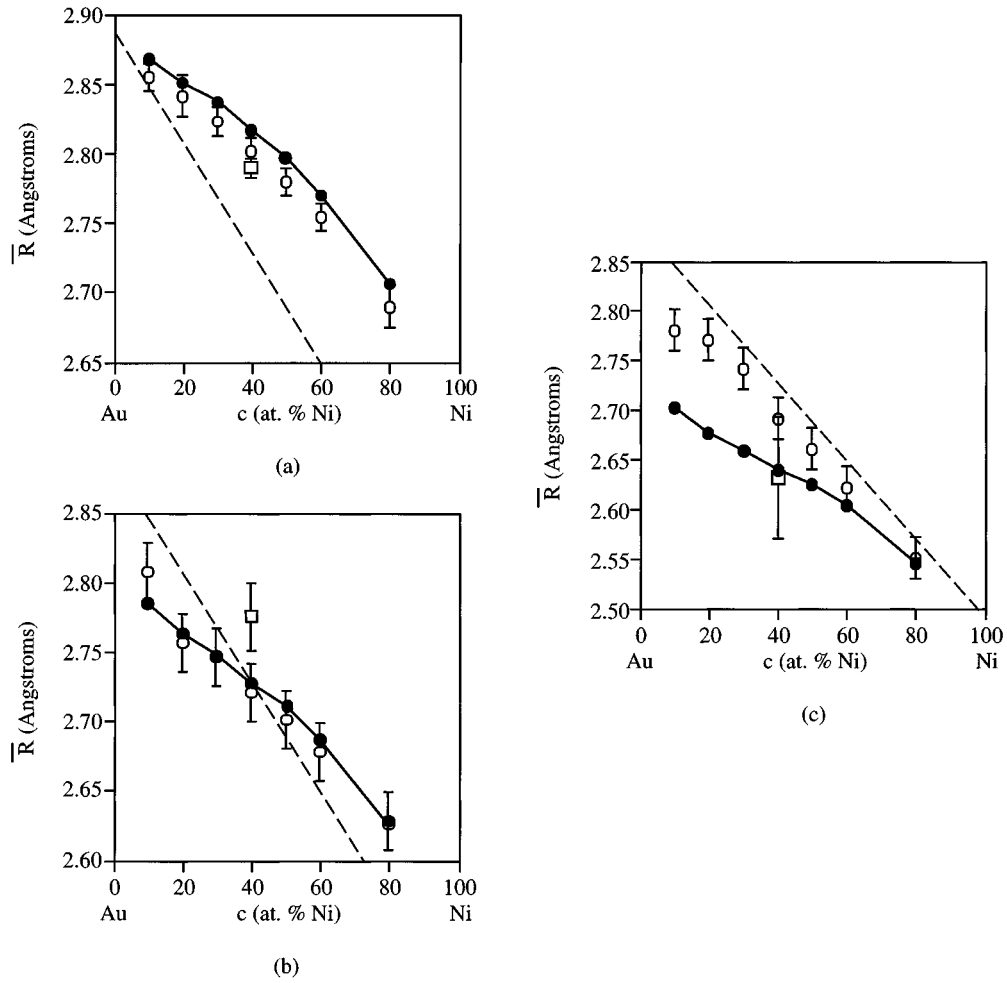

FIG. 5. Calculated and experimentally measured values of the average bond lengths ($\bar{R}$) as a function of alloy composition for nearest-neighbor Au-Au (a), Au-Ni (b), and Ni-Ni (c) bonds in Au-Ni solid solutions. The solid circles are results of the calculations discussed in the text; the solid lines connecting the solid-circles are merely drawn as a guide to the eye. EXAFS (Ref. 32) and diffuse x-ray scattering (Ref. 30) experimental results are plotted with open circles and squares, respectively.

In addition to the approximations made in deriving the SOE expressions for the alloy energy and vibrational free energy, an additional source of error introduced in the MF-SOE approach is the use of the MF approximation in the calculation of alloy thermodynamic properties and PCF's (SRO parameters). In the calculation of PCF's, the MF-KCM expression given in Eq. (9) has been shown to qualitatively fail in some cases.[22] As discussed in detail in Sec. III D, in the present study errors associated with the MF theory were found to be much less severe for the calculated PCF's of a Au–40 at. % Ni alloy. In particular, the position of the peak in the PCF in reciprocal space was computed to be roughly half way between the Γ and X special points of the fcc Brillouin zone in both MF and MC calculations; the MC- and MF-calculated peak positions for the PCF in reciprocal space were only slightly displaced from one another.

For Ising (and, equivalently, lattice-gas) model Hamiltonians with short-ranged interactions, the errors associated with the MF approximation for the calculation of thermodynamic properties and c-T phase diagrams have been well established. Specifically, for phase-separating alloys with fcc structures (such as those considered here) and energetics described by the nearest-neighbor ferromagnetic Ising model, the MF approximation leads to approximately a 23% overestimation of the calculated value of T_c.[1] In the present study, the alloy Hamiltonian is somewhat more complex than that of the nearest-neighbor Ising model. Specifically, the SOE Hamiltonian contains longer-ranged pair interactions as well as a composition-dependent term E_0. As a consequence, the estimates of the accuracy of the MF approximation obtained for short-ranged Ising Hamiltonians are not directly relevant for our calculations. In particular, in the limiting case where the magnitudes of the EPI's are small enough that the sum of the interaction terms $V(\mathbf{k})\langle\delta c(\mathbf{k})\delta c^*(\mathbf{k})\rangle$ is negligible compared to the term E_0 in Eq. (6), the MF expression for the alloy free energy given in Eq. (8) is exact.

In Sec. III C the accuracy of the MF approximation for the calculation of c-T phase diagrams in the present study was assessed by comparing results obtained using both MF and MC methods. The MF-calculated values of the transition temperatures for Cu-Ni were overestimated at some compositions by as much as 20%, an error comparable in magnitude to that found for the nearest-neighbor ferromagnetic Ising model. However, in the case of Cu-Ag alloys, the MF errors were found to be much smaller and phase transition temperatures were overestimated by at most 3%. These re-

sults for Cu-Ni and Cu-Ag demonstrate that in general the accuracy of the MF approximation in the calculation of alloy thermodynamic properties is system dependent.

B. Structural and thermodynamic properties of alloy solid solutions

With the SOE method we have analyzed the effects which static and dynamic atomic displacements have on the structural and thermodynamic properties of Cu-Ni, Cu-Ag, and Au-Ni solid solutions. In Sec. II we discuss how, within the SOE formalism, static displacements give rise to a relaxation-energy contribution to the enthalpy of an alloy solid solution. The magnitude of the relaxation energy has been calculated by a variety of techniques in a number of first-principles computational studies (see Refs. 3, 5, 9, 13, 15, 16, 25, 26, and 34–36 as well as references cited therein) of the energetics of disordered alloys. In agreement with the findings of these previous studies, the results displayed in Fig. 2 for Cu-Ag and Au-Ni alloys clearly show that the relaxation energy can amount to a sizable fraction of the heat of mixing in alloys displaying large degrees of atomic-size mismatch.

The effect of static and dynamic (vibrational) atomic displacements on the thermodynamic stability of alloy solid solutions was discussed in Sec. III C. It was shown that the relaxation energy associated with static displacements led to as much as 31% lowering of the calculated values of phase transition temperatures. In the cases of Cu-Ni and Cu-Ag, results displayed in Fig. 2 illustrate that vibrational contributions to the alloy free energy were found to have effects on calculated phase diagrams which are comparatively smaller than those arising from static atomic relaxations. In particular, for Cu-Ni the main effect of vibrations was to shift the top of the calculated miscibility gap to higher Ni compositions. For Cu-Ag vibrational effects were found to be responsible for a slight increase in the solubility limits below the eutectic temperature. The effect of vibrational free-energy contributions on the results of phase-diagram calculations for phase-separating metallic,[13,16] semiconductor,[17] and ceramic[18] alloy systems also has been analyzed in previous studies. In each of these it was found that vibrational contributions lowered the critical phase-separation temperature by amounts ranging from between a few percent[17] to as much as 15%.[13,16,18] Additionally, it has been found that the effects upon calculated phase diagrams attributed to vibrational free energies can be significantly asymmetric in nature, as we find for Cu-Ni.

The results shown in Fig. 3 and discussed in Sec. III D provide an interesting example which illustrates how chemical and displacive contributions to the energy can compete in determining the atomic structure of an alloy solid solution. Specifically, for Au–40 at. % Ni alloys we find that clustering SRO is favored by the relaxation energy, while chemical interactions prefer ⟨100⟩-type order. The result of this competition is SRO intermediate between these two opposite extremes.

Wu and Cohen[44] have also studied the origin of SRO in Au-Ni using a SOE approach based upon the formalism of Cook and de Fontaine.[2] In this formalism, which is derived using the ''host'' reference frame described in Sec. II A, there are three contributions to the EPI. The first two, which are associated with chemical and relaxation-energy contributions to the energy, are comparable to those introduced in Sec. II. The third arises from the elastic ''unrelaxed energy'' (UE), which is defined as the elastic work required to form a disordered alloy of size-mismatched atoms located on ideal lattice sites. The parameters in the Cook–de Fontaine SOE formulas were parametrized by Wu and Cohen using neutron inelastic[48] as well as diffuse scattering[41] data. It was found that the total elastic-energy contribution to $V(\mathbf{k})$, given by the sum of the UE and the relaxation energy, has a minimum at $\mathbf{k}=\langle 0.6,0,0\rangle$. They therefore propose that the elastic energy alone is responsible for a minimum in the total value of $V(\mathbf{k})$ and a corresponding peak in the SRO at this position in reciprocal space. Furthermore, they suggest that the minimum in the elastic-energy component of $V(\mathbf{k})$ can be attributed to the nature of the force constants in the system which are known to give rise to a softening of the phonon spectrum at $\mathbf{k}=\langle 0.6,0,0\rangle$.[48] The elastic UE is contained within the E_0 term in our formalism, and it does not contribute directly to our $V(\mathbf{k})$ due to the different reference frame used in our SOE method as compared with that of Cook and de Fontaine. Consequently, it is difficult for us to comment directly on the explanation proposed by Wu and Cohen. However, it is worth noting that Wu and Cohen find minima in the chemical and relaxation-energy contributions to $V(\mathbf{k})$ which occur near $\mathbf{k}=\langle 1,0,0\rangle$ and at $\mathbf{k}=\langle 0,0,0\rangle$, respectively, in qualitative agreement with the results of the present study. In our opinion further work is warranted to establish the possible connection between phonon softening and a minimum in $V(\mathbf{k})$ near $\mathbf{k}=\langle 0.6,0,0\rangle$.

Our results (see Sec. II D) which demonstrate that relaxation-energy contributions to the EPI act to drag the peak in the SRO away from Brillouin-zone-boundary special points is a general one which is not unique to the Au-Ni system. Specifically, we show in the Appendix how symmetry considerations allow us to conclude that the second term on the right-hand side of Eq. (4), $P(\mathbf{k})=-\psi(\mathbf{k})\phi^{-1}(\mathbf{k})\psi^{*}(\mathbf{k})$, takes on a maximum value (equal to zero) at each of the special points excluding Γ. Therefore, within the KCM theory, the term $P(\mathbf{k})$ can only act to displace the peak in the PCF away from the Brillouin zone boundary when special-point-ordering SRO is favored chemically. In practice, whether or not the relaxation energy actually does displace the SRO peak in such situations is dependent upon the relative magnitudes of the chemical and relaxation-energy contributions to the EPI. In Au-Ni these contributions are of similar magnitude, as shown in Fig. 3(c), and it is likely that this may be the case in other alloy systems as well.

ACKNOWLEDGMENTS

Helpful discussions with Dr. Jeff Althoff, Dr. Duane Johnson, Dr. Andrew Quong, Dr. Chris Wolverton, Dr. Alex Zunger, and Professor Didier de Fontaine are gratefully acknowledged. We would also like to thank Dr. Z. W. Lu for providing us with his calculated values of formation energies for Au-Ni alloy compounds prior to their publication. This research was supported by the U.S. Department of Energy, Office of Basic Energy Sciences, Materials Science Division, under Contract No. DE-AC04-94AL85000.

APPENDIX: EFFECT OF DISPLACEMENTS ON SRO

In this appendix we give a proof that the relaxation-energy contribution to $V(\mathbf{k})$ is maximal at all special points excluding Γ. The first element of the proof relies on the fact that this contribution has a quadratic form $P(\mathbf{k}) \equiv -[\psi_\alpha(\mathbf{k})\phi^{-1}_{\alpha,\beta}(\mathbf{k})\psi^*_\beta(\mathbf{k})]$. For a stable crystal, $\phi(\mathbf{k})$ and $\phi^{-1}(\mathbf{k})$ are positive-definite matrices, except at $\mathbf{k}=0$. Consequently, for $\mathbf{k}\neq 0$, $P(\mathbf{k})\leqslant 0$, where the equality holds when $\psi(\mathbf{k})=0$. In other words, for all $\mathbf{k}\neq 0$, $P(\mathbf{k})$ takes on its maximum possible value, zero, whenever $\psi(\mathbf{k})=0$.

From the symmetry of the reference state, it can be shown that for every symmetry element S which is a member of the point group of the parent lattice, $\psi(\mathbf{R})$ transforms as

$$S\{\psi_1(\mathbf{R}),\psi_2(\mathbf{R}),\psi_3(\mathbf{R})\}=\{\psi_1(S\mathbf{R}),\psi_2(S\mathbf{R}),\psi_3(S\mathbf{R})\} \tag{A1}$$

or $S\psi(\mathbf{R})=\psi(S\mathbf{R})$, for short. As a consequence, it is straightforward to show that the following relation holds for the Fourier-transformed values of ψ:

$$S\psi(\mathbf{k})=\psi(S\mathbf{k}). \tag{A2}$$

Consider now a $\mathbf{k}$ vector $\mathbf{k}^*$ and a symmetry element S^* for which the following relation holds: $S^*\mathbf{k}^*=\mathbf{k}^*+\mathbf{G}$, where $\mathbf{G}$ is a reciprocal lattice vector. By translational symmetry and the relation (A2), it follows that $S^*\psi(\mathbf{k}^*)=\psi(\mathbf{k}^*)$. As a consequence, the vector $\{\psi_1(\mathbf{k}^*),\psi_2(\mathbf{k}^*),\psi_3(\mathbf{k}^*)\}$ must lie along or within the symmetry element S^*. The set of symmetry operations $\{S^*\}$ for which $S^*\mathbf{k}^*=\mathbf{k}^*+\mathbf{G}$ holds can be shown to form a group[49] referred to as the point group of $\mathbf{k}^*$. If two or more elements in the point group of $\mathbf{k}^*$ intersect at a common point, it follows that $\psi(\mathbf{k}^*)=0$. The points in reciprocal space for which this latter requirement is true are the special points (see, for example, Ref. 3).

To summarize, for each of the special points $\mathbf{k}^*$, $\psi(\mathbf{k}^*)$ vanishes owing to the symmetry properties (A1) and (A2). For all special points $\mathbf{k}^*$ except Γ, this implies that $P(\mathbf{k}) \equiv -[\psi_\alpha(\mathbf{k})\phi^{-1}_{\alpha,\beta}(\mathbf{k})\psi^*_\beta(\mathbf{k})]$ takes on its maximum value of zero.

[1] D. de Fontaine, Solid State Phys. **34**, 74 (1979).
[2] H. E. Cook and D. de Fontaine, Acta Metall. **17**, 915 (1969).
[3] D. de Fontaine, Solid State Phys. **47**, 33 (1994).
[4] A. G. Khatchaturyan, *The Theory of Structural Transformations in Solids* (Wiley, New York, 1983).
[5] A. Zunger, in *Statics and Dynamics of Alloy Phase Transformations*, edited by P. E. A. Turchi and A. Gonis, Vol. 319 of NATO Advanced Study Institute, Series B: Physics (Plenum, New York, 1994).
[6] F. Ducastelle, *Order and Phase Stability in Alloys* (North-Holland, New York, 1991).
[7] G. M. Stocks, D. M. C. Nicholson, W. A. Shelton, B. L. Gyorffy, F. J. Pinski, D. D. Johnson, J. B. Staunton, B. Ginatempo, P. E. A. Turchi, and M. Sluiter, in *Statics and Dynamics of Alloy Phase Transformations* (Ref. 5); J. D. Althoff, D. D. Johnson, and F. J. Pinski, Phys. Rev. Lett. **74**, 138 (1995).
[8] A. Gonis, X.-G. Zhang, A. J. Freeman, P. E. A. Turchi, G. M. Stocks, and D. M. C. Nicholson, Phys. Rev. B **36**, 4630 (1987).
[9] S. de Gironcoli, P. Giannozzi, and S. Baroni, Phys. Rev. Lett. **66**, 2116 (1991); N. Marzari, S. de Gironcoli, and S. Baroni, *ibid*. **72**, 4001 (1994).
[10] M. S. Daw and M. I. Baskes, Phys. Rev. Lett. **50**, 1285 (1983); Phys. Rev. B **29**, 6443 (1984).
[11] M. S. Daw, S. M. Foiles, and M. I. Baskes, Mater. Sci. Rep. **9**, 251 (1993); S. M. Foiles, in *Equilibrium Structure and Properties of Surfaces and Interfaces*, edited by A. Gonis and G. M. Stocks, Vol. 300 of NATO Advanced Study Institute, Series B: Physics (Plenum, New York, 1992).
[12] *Monte-Carlo Methods in Statistical Physics*, edited by K. Binder, Topics in Current Physics Series Vol. 7 (Springer-Verlag, New York, 1986); *Applications of the Monte Carlo Method in Statistical Physics*, edited by K. Binder, Topics in Current Physics Series Vol. 36 (Springer-Verlag, New York, 1986).
[13] J. M. Sanchez, J. P. Stark, and V. L. Moruzzi, Phys. Rev. B **44**, 5411 (1991).
[14] G. D. Garbulsky and G. Ceder, Phys. Rev. B **49**, 327 (1994).
[15] A. Chiolero, Ph.D. thesis, Institut de Physique Théorique, Université de Fribourg, 1995.
[16] C. Colinet, J. Eymery, A. Pasturel, A. T. Paxton, and M. van Schilfgaarde, J. Phys. Condens. Matter **6**, L47 (1994).
[17] A. Silverman, A. Zunger, R. Kalish, and J. Adler, Phys. Rev. B **51**, 10 795 (1995).
[18] P. D. Tepesch, A. F. Kohan, G. D. Garbulsky, G. Ceder, C. Coley, H. T. Stokes, L. L. Boyer, M. J. Mehl, B. P. Burton, K. Cho, and J. Joannopoulos (unpublished).
[19] L. Anthony, J. K. Okamoto, and B. Fultz, Phys. Rev. Lett. **70**, 1128 (1993); L. Anthony, L. J. Nagel, J. K. Okamoto, and B. Fultz, *ibid*. **73**, 3034 (1994).
[20] M. A. Krivoglaz, *Theory of X-Ray and Thermal-Neutron Scattering by Real Crystals* (Plenum, New York, 1969).
[21] P. C. Clapp and S. C. Moss, Phys. Rev. **142**, 418 (1966); L. Reinhard and S. C. Moss, Ultramicroscopy **52**, 223 (1993).
[22] F. Solal, R. Caudron, F. Ducastelle, A. Finel, and A. Loiseau, Phys. Rev. Lett. **58**, 2245 (1987); C. Wolverton and Alex Zunger, Phys. Rev. B **51**, 6876 (1995).
[23] S. M. Foiles, Phys. Rev. B **32**, 7685 (1985).
[24] *Selected Values of Thermodynamic Properties of Metals and Alloys*, edited by R. R. Hultgren, P. D. Anderson and K. K. Kelley (Wiley, New York, 1963).
[25] S.-H. Wei, A. A. Mbaye, L. G. Ferreira, and Alex Zunger, Phys. Rev. B **36**, 4163 (1987).
[26] Z. W. Lu and A. Zunger, Phys. Rev. B **50**, 6626 (1994).
[27] R. Najafabadi, H. Y. Wang, D. J. Srolovitz, and R. LeSar, Acta Metall. Mater. **39**, 3071 (1991).
[28] R. LeSar, R. Najafabadi, and D. J. Srolovitz, Phys. Rev. Lett. **63**, 624 (1989).
[29] R. Najafabadi, D. J. Srolovitz, E. Ma, and M. Atzmon, J. Appl. Phys. **74**, 3144 (1993).
[30] In the calculations for Cu-Ag performed in Ref. 29, Najafabadi *et al.* used the set of EAM potentials described in the following reference: S. M. Foiles, M. I. Baskes, and M. S. Daw, Phys. Rev. B **33**, 7983 (1986). In our own calculations, which were performed for the purpose of comparing with the results of Ref. 29, we also used this same set of potentials. For the rest of the calculations presented in this paper, however, use was made of a

different set of Cu-Ag potentials which were derived according to the method described in Sec. II C.

[31] P. Soven, Phys. Rev. **67**, 107 (1967).

[32] The displacement corrections to the CW method are presently being implemented by J. D. Althoff and D. D. Johnson (unpublished).

[33] M. H. F. Sluiter, D. de Fontaine, X. Q. Guo, R. Podloucky, and A. J. Freeman, Phys. Rev. B **42**, 10 460 (1990).

[34] C. Amador, W. R. L. Lambrecht, M. van Schilfgaarde, and B. Segall, Phys. Rev. B **47**, 15 276 (1993).

[35] D. B. Laks, L. G. Ferreira, S. Froyen, and A. Zunger, Phys. Rev. B **46**, 12 587 (1992).

[36] C. Amador and G. Bozzolo, Phys. Rev. B **49**, 512 (1994).

[37] W. H. Press, B. P. Flannery, S. A. Teukolsky, and W. T. Vetterling, *Numerical Recipes: The Art of Scientific Computing* (Cambridge University Press, New York, 1989).

[38] K. Terakura, T. Oguchi, T. Mohri, and K. Watanabe, Phys. Rev. B **35**, 2169 (1987).

[39] *Binary Alloy Phase Diagrams*, 2nd ed., edited by T. B. Massalski, H. Okamoto, P. R. Subramanian, and L. Kacprzak (ASM International, Materials Park, OH, 1990).

[40] In the case of Cu-Ag, this result is consistent with the experimental finding that these alloys remain immiscible up to the eutectic temperature. Au-Ni alloys, however, show complete miscibility at temperatures below the solidus. Therefore, our calculated result that Au-Ni alloys are dynamically unstable at temperatures below the unmixing temperature (T_c) is in disagreement with experimental findings. This discrepancy with experimental observations for Au-Ni is largely due to the approximations we have used in calculating the vibrational free energy. We have found that in alloy systems (such as Au-Ni) where atomic displacements are large, the approximate vibrational free-energy expression given by Eq. (7) sometimes gives rise to lattice instabilities for temperatures at which relaxed random alloys should be stable according to the results of ''exact'' supercell calculations. We believe that this problem with our approximate treatment of atomic vibrations originates from the fact that the dynamical matrix $\phi(\mathbf{k})$ in Eq. (7) is derived for a random alloy with unrelaxed rather than relaxed atomic positions.

[41] T. B. Wu and J. B. Cohen, Acta Metall. Mater. **31**, 1929 (1983).

[42] P. A. Flinn, B. L. Averbach, and M. Cohen, Acta Metall. **1**, 664 (1953).

[43] D. de Fontaine and H. E. Cook, in *Critical Phenomena in Alloys and Superconductors*, edited by R. E. Mills, E. Ascher, and R. I. Jaffee (McGraw-Hill, New York, 1971), p. 257.

[44] T. B. Wu and J. B. Cohen, Acta Metall. **32**, 861 (1984).

[45] G. Renaud, N. Motta, F. Lançon, and M. Belakhovsky, Phys. Rev. B **38**, 5944 (1988).

[46] C. Amador and D. de Fontaine (private communication).

[47] As a specific example, the third-order term $[\Sigma_k(\partial^3 E/\partial u_i \partial u_j \partial c_k)\,\delta c_k]$ gives rise to a configurationally dependent contribution to the force constant matrix of an alloy; this and other higher-order terms are neglected in the approach described in Sec. II B.

[48] T. B. Wu, J. B. Cohen, and W. Yelon, Acta Metall. **30**, 2065 (1982).

[49] L. M. Falicov, *Group Theory and Its Physical Applications* (University of Chicago Press, Chicago, 1966).